

Fast Accurate Defect Detection in Wafer Fabrication

Thomas Olschewski*, Technische Universität Dresden

August 27, 2021

Abstract

A generic fast method for object classification is proposed. In addition, a method for dimensional reduction is presented. The presented algorithms have been applied to real-world data from chip fabrication successfully to the task of predicting defect states of tens of thousands of chips of several products based on measurements or even just part of measurements. Unlike typical neural networks with a large number of weights to optimize over, the presented algorithm tries optimizing only over a very small number of variables in order to increase chances to find a global optimum. Our approach is interesting in that it is fast, led to good to very good performance with real-world wafer data, allows for short implementations and computes values which have a clear meaning easy to explain.

*thomas.olschewski@tu-dresden.de

Contents

| | | |
|----------|---|-----------|
| 1 | Acknowledgements | 2 |
| 2 | Introduction | 2 |
| 2.1 | Overview | 4 |
| 3 | The Algorithms | 5 |
| 3.1 | Definitions | 5 |
| 3.2 | Dense Formulation | 5 |
| 3.2.1 | Extensions | 6 |
| 3.3 | $s(\cdot, y)$ as a Linear Functional | 6 |
| 3.4 | Machine Learning | 7 |
| 3.4.1 | The General Algorithm | 7 |
| 3.4.2 | Scaling | 8 |
| 3.4.3 | Computing Predictions | 9 |
| 3.4.4 | Cutoff Selection | 9 |
| 3.4.5 | Refined Method For Cutoff Selection | 10 |
| 3.5 | Settings of Practical Applications | 12 |
| 3.6 | Application 1: Identification of Positive Objects | 12 |
| 3.6.1 | Building and Solving a System of Implications | 13 |
| 3.7 | Application 2: Predicting Positive Objects | 14 |
| 4 | Experimental Setup | 19 |
| 4.1 | The Task | 19 |
| 4.2 | The Implementation | 20 |
| 5 | Results | 21 |
| 5.1 | Properties | 21 |
| 5.2 | Free Parameters | 21 |
| 5.3 | Results for Application 2 | 22 |
| 5.3.1 | Predicting Specific Types of Failure | 27 |
| 5.3.2 | Detecting Iris Type | 27 |
| 5.3.3 | Prototypical Positive Objects | 28 |
| 5.3.4 | Predicting Defect States Knowing Only Part of Measure- ment Data | 31 |
| 5.3.5 | Dimensional Reduction | 36 |
| 6 | Conclusion | 39 |

1 Acknowledgements

I thank Zoltán Sasvári for providing the environment which made this research possible, for carefully reading the manuscript and for some corrections.

Research leading to these results has received funding from the iRel40 project. iRel40 is a European co-funded innovation project that has been granted by the **ECSEL** Joint Undertaking (JU) under grant agreement n° **876659**. The funding of the project comes from the Horizon 2020 research programme and participating countries. National funding is provided by Germany, including the Free States of Saxony and Thuringia, Austria, Belgium, Finland, France, Italy, the Netherlands, Slovakia, Spain, Sweden, and Turkey.

Disclaimer: The document reflects only the author’s view and the JU is not responsible for any use that may be made of the information it contains.



2 Introduction

In this paper we propose a generic fast method for object classification some specialisations of which serve to detect anomalies in measurement data of wafer fabrication. The basic task of this application is predicting the positive/negative state of objects knowing only measurement data. In the wafer data application this translates to predicting from measurement data early in the fabrication whether some chip will turn out to be defective—i.e. is a positive object or not—later.

Our approach is interesting in that it is fast, led to good to very good performance with real-world wafer data, allows for short implementations and computes values which have a clear meaning easy to explain.

The baselining principles are using thresholdings of coordinate-wise normalized data in order to derive bit patterns from the input data, computing similarities to a small set of training objects known to be positive and finding an optimal cutoff in order to classify objects yet unknown. We propose a selection of thresholdings and similarity measures which have been proven successful in the wafer data application. In its basic form there is one free parameter t for which good value selections can be obtained easily.

We show how this method for object classification follows from a logical algorithm tackling a somewhat easier problem, the problem of object identification, i.e. the problem of deciding whether some object belongs to a known set of (training) objects.

We point out that in several practical settings our algorithms allow for identifying *prototypical defect chips* which in our nomenclature are chips being es-

pecially important in the sense that they possess properties which allow for accurately classifying lots of other, yet unclassified, chips.

Furthermore we propose a fast method for reducing input data dimensionality which serves as an optional preprocessing step.

Time and space complexities of our algorithms are quasi-linear and thus are good-natured enough in order to allow for classifying large sets of objects with high-dimensional input data on normal PC hardware. In our applications we could classify e.g. 11328 chips in 915 dimensions with accuracy 99.8% and kappa 0.979 within a few seconds.

The algorithm we describe here possesses several advantages over typical usage of neural nets for machine learning by back-propagation [9]. Firstly, in our applications there is only a very limited number of unknowns to be optimized over, namely the parameter t of subsection 3.5 being used in thresholding the input data and thus implicitly contained in Algorithm 1, and the cut-off C in Algorithm 3 which converts the guesses into a binary positive/negative prediction.

So, unlike with back-propagation we are not faced with thousands or even millions of unknown weights spanning a giant search range to be optimized over but with only one or two which enables approximating the global optimum for arbitrary measures of prediction quality. With our methods, it is not hopeless to try finding a global optimum in reasonable time on ordinary PC hardware as the graphs of target functions are rather good-natured having few local optima. Secondly, the algorithmic meaning of the few unknowns in our algorithms is easy to understand which we see as a step towards XAI (explainable AI), see for example [2].

The goals of a series of ongoing research projects for improving quality control in chip fabrication suggest the following properties for an ideal algorithm in order to be economically useful:

1. Not requiring Gaussian distribution of single—or several or all—parameters.
2. High true-positive-false-positive quotients (TP/FP): As few as possible good devices shall be scrapped for sorting out bad devices.
3. High efficiency: Data should be processed in fabrication real-time.
4. Ability of coping with large amount of data: One typical lot $\approx 30 - 100$ MiB of data.
5. Reducing the number of tests: Measurements are costly and time consuming to different extents so it is desirable to need less of them without reducing the quality of defect prediction.

Algorithms 3 and 4 which will be presented in subsection 5.1 meet all of these goals.

2.1 Overview

The rest of this paper is organized as follows. In section 3 we will describe our algorithms and two applications. Section 4 is about the experimental setup and the task to be solved. In section 5 we will evaluate and analyse the results we obtained from a larger number of test runs and describe a method for dimensional reduction applied successfully. In section 6 we will add concluding thoughts.

3 The Algorithms

3.1 Definitions

Let $B_i \subseteq B$, $i = 1, \dots, s$ be subsets of a fixed base set B with characteristic functions $\mathbb{1}_{B_i}$. We define $P_i = \mathbb{1}_{B_i}$ for shortness and $\mathbb{P} = (P_1, \dots, P_s)$. For every $x \in B$ define $I(x) = \{i \mid x \in B_i\}$. For every pair $x, y \in B$ we define

$$s(x, y) = \begin{cases} \frac{|I(x) \cap I(y)|}{|I(x)|} & I(x) \neq \emptyset \\ 0 & I(x) = \emptyset \end{cases}$$

and call it *coincidence index* of x and y . Clearly, $0 \leq s(x, y) \leq 1$ where 0 means disjointness of $I(x)$ and $I(y)$ and 1 means $I(x) \subseteq I(y)$.

Let $D \subseteq B$ be a set henceforth called *data points* and $T \subseteq D$ a set henceforth called *training set*.

In what follows we will use the following abbreviation:

$$\mathbb{B} = \{0, 1\}$$

3.2 Dense Formulation

Alternatively, the formula for the coincidence index can be rewritten by using incidence vectors as follows:

$$s(x, y) = \frac{\sum_{i=1}^s P_i(x) \cdot P_i(y)}{\sum_{i=1}^s P_i(x)} \quad (x, y \in B)$$

We set $s(x, y) = 0$ in case $\sum_{i=1}^s P_i(x) = 0$. We call

$$v(x) = (P_1(x), \dots, P_s(x)) \in \mathbb{B}^s$$

the *incidence vector* of x relative to \mathbb{P} . Then we can write

$$s(x, y) = \frac{v(x) \cdot v(y)}{v(x) \cdot v(x)} \quad (x, y \in B)$$

with $a \cdot b$ being the inner product, computed in \mathbb{N} , of two 0-1 vectors a, b .

We can rewrite this further as

$$s(x, y) = \frac{H(v(x) \circ v(y))}{H(v(x))} \quad (x, y \in B)$$

where $H(v)$ is the Hamming weight

$$H(v) = \sum_{i=1}^s v_i$$

of vector $v \in \mathbb{B}^s$ ($H(v) \in \{0, \dots, s\}$) and $v \circ w = (v_1 \cdot w_1, \dots, v_s \cdot w_s)$ shall denote the component-wise multiplication of two vectors v and w . If limited to 0-1 vectors v and w , $v \circ w = (v_1 \wedge w_1, \dots, v_s \wedge w_s)$ and

$$H(v \circ w) = |\{i \mid v_i = w_i = 1\}|.$$

Now we consider the following problem.

Given: A base set B , data set $D \subseteq B$, training set $T \subseteq B$, sets $B_i \subseteq B$, $i = 1, \dots, s$, and a data point $x \in D$.

Task: Compute

$$s(x, T) = \max\{s(x, y) \mid y \in T\}.$$

We call $s(x, T)$ the *coincidence index of x relative to T* . Since $s(x, T) = 1$ trivially if $x \in T$ we will consider only data points $x \notin T$ henceforth.

Computability assumptions. The predicates $P_i : B \rightarrow \mathbb{B}$ must be computable in the machine model used, elements of B must be representable in that machine model. See, for example, [10] for an introduction to these topics.

Examples. Machine model = Turing machine and $B = \mathbb{Q}^n$. B_i must be Turing decidable sets in this case.

3.2.1 Extensions

$s(x, y)$ is not limited to the coincidence index as defined in subsection 3.1. Basically, if $f : \mathbb{B}^s \times \mathbb{B}^s \rightarrow [0, 1] \subseteq \mathbb{Q}$ is any function expressing a degree of similarity of two 0-1 vectors in some sense then we can set

$$s(x, y) = f(v(x), v(y)).$$

Cohen's kappa function is another example for f we used in practice, see subsection 3.4.4 for a definition.

In addition, $s(x, T)$ can be substituted by other functions which promise to indicate a spread in between positive and negative objects. For example, we investigated $s(x, T) = \min\{s(x, y) \mid y \in T\}$, too.

3.3 $s(\cdot, y)$ as a Linear Functional

With x —and thus $v(x)$ —being fixed, $s(x, y)$ can be written as a linear functional in the vector $v(y)$. For, by setting

$$L_x(a) = \frac{v(x) \cdot a}{H(v(x))}$$

we can write

$$s(x, y) = L_x(v(y))$$

where $v \cdot w$ is the euclidian inner product and $H(\cdot)$ is the Hamming weight function.

Using the formula for “cosine similarity” of 0-1 vectors $v(x), v(y)$

$$C(v(x), v(y)) = \frac{v(x) \cdot v(y)}{\|v(x)\| \cdot \|v(y)\|}$$

and using

$$\|v\| = H(v)^{1/2}$$

for 0-1 vectors v with the euclidian distance $\|\cdot\|$ we can write

$$\begin{aligned} s(x, y) &= L_x(v(y)) = \frac{v(x) \cdot v(y)}{H(v(x))} \\ &= \frac{v(x) \cdot v(y)}{H(v(x))^{1/2} \cdot H(v(y))^{1/2}} \cdot \frac{H(v(y))^{1/2}}{H(v(x))^{1/2}} \\ &= C(v(x), v(y)) \cdot \frac{H(v(y))^{1/2}}{H(v(x))^{1/2}} \end{aligned}$$

So $s(x, y)$ is the “cosine similarity” of 0-1 vectors $v(x), v(y)$, multiplied by

$$q(x, y) = \frac{H(v(y))^{1/2}}{H(v(x))^{1/2}}$$

3.4 Machine Learning

We extend the above setup by a function

$$p : D \rightarrow \mathbb{B}$$

which assigns one bit $p(x)$ to every data point $x \in D$. We call x a *positive* data point if $p(x) = 1$ and a *negative* data point if $p(x) = 0$. Let

$$D^1 = \{x \in D \mid p(x) = 1\}, \quad D^0 = \{x \in D \mid p(x) = 0\}$$

We limit ourselves to considering exclusively positive data points for being used as training data, i.e. in what follows we presuppose

$$T \subseteq D^1$$

3.4.1 The General Algorithm

Let $B \subseteq \mathbb{R}^n$ and $D \subseteq B$ be a set of data points.


```

Input:  $B = \mathbb{R}^n$ ,  $D \subseteq B$ ,  $p \in [0, 100]$ 
1 scale( $D$ )
2  $T = \text{select}(p, D^1)$ 
3 if  $T = \emptyset$  then
4   | stop
5 end
6 for  $x \in D \setminus T$  do
7   | compute  $s(x, T)$ 
8 end
9  $Av^0 := \text{avg}\{s(x, T) \mid x \in D^0\}$ 
10  $Av^1 := \text{avg}\{s(x, T) \mid x \in D^1\}$ 

```

Algorithm 1: General algorithm

$\text{select}(p, M)$ is a function which draws

$$\lceil |M| \cdot \frac{p}{100} \rceil$$

elements from a set M randomly without repetition and $s(x, T)$ is as described above. Here—and in other places—we neglect the trivial case of T being empty. $\text{scale}(D)$ refers to the following function.

3.4.2 Scaling

```

Input/Output:  $D = \{x_1, \dots, x_m\} \subseteq \mathbb{R}^n$ 
1 for  $j = 1 \dots n$  do
2   | compute  $\mu_j, \sigma_j$ 
   | // mean and standard deviation of the  $j$ -th components of  $x_1, \dots, x_m$ 
3 end
4 for  $i = 1 \dots m$  do
5   | for  $j = 1 \dots n$  do
6     |  $x_{i,j} := \begin{cases} \frac{x_{i,j} - \mu_j}{\sigma_j}, & \sigma_j \neq 0 \\ 0, & \sigma_j = 0 \end{cases}$ 
7   | end
8 end

```

Algorithm 2: $\text{scale}(D)$

D has mean 0 and standard deviation 1 after scaling. After scaling D the general algorithm does not operate on the data points $x_i = (x_{i,1}, \dots, x_{i,n})$ actually given but on the vectors that quantify how far (by how many standard deviations σ_j) $x_{i,j}$ is away from the mean μ_j .

3.4.3 Computing Predictions

Let B , D , p and T the same as in Algorithm 1.

Input: $s(x, T)$ as computed by Algorithm 1, $C \geq 0$

```

1 for  $x \in D \setminus T$  do
2    $F(x, T, C) := \begin{cases} 1, & s(x, T) \geq C \\ 0, & s(x, T) < C \end{cases}$ 
3 end
```

Algorithm 3: Computing predictions

C operates as a cutoff for digitizing $s(x, T)$. There is a wide range of methods which can be used for specifying C of which we describe just two.

3.4.4 Cutoff Selection

In what follows, we assume $Av^1 - Av^0 \geq 0^1$ for Av^1, Av^0 as defined in Algorithm 1.

Naïve cutoff selection.

$$C := \frac{Av^1 - Av^0}{2}$$

This is a better-than-nothing selection which can be computed very fast but may deliver predictions $F(x, T, C)$ far from what can be achieved with a more sophisticated cutoff.

Optimizing cutoff for some statistical quantity $Q(v, w)$.

Let $D \setminus T = x^1, \dots, x^{m^*}$ an enumeration in some fixed order and

$$S = (p(x^1), \dots, p(x^{m^*}))$$

the 0-1 vector of their positive/negative states. Let be

$$F(C) = (F(x^1, T, C), \dots, F(x^{m^*}, T, C))$$

the 0-1 vector of all $F(x, T, C)$ for $x \in D \setminus T$ in the same ordering as in S . Furthermore let be $Q(v, w)$ some statistical quantity which represents some measure of similarity of two 0-1 vectors v and w , such like accuracy² or Cohen's

¹If this does not hold true in a specific application then one can replace $F(x, T, C)$ by its logical inverse $\neg F(x, T, C) = 1 - F(x, T, C)$ in order to achieve $Av^1 - Av^0 \geq 0$. We would interpret this as an indication of an insufficient training set T —it may be too small, containing too few characteristic samples, or samples not characteristic enough— or that this algorithm is not apt to this specific input data B , D , p and the set of predicates \mathbb{P} .

²Accuracy is the amount of coincident bits: $\text{accu}(v, w) = \frac{1}{n} \cdot \sum_{i=1}^n (v_i \cdot w_i + (1-v_i)(1-w_i))$.

kappa³

Input: B, D, T, p as in Algorithm 1

```

1 for  $C$  on a grid  $\mathcal{C} \subset [0, 1]$  do
2   |   Compute  $F(C)$  by Algorithm 3
3   |   Compute  $Q(F(C), S)$ 
4 end
5  $Q_{opt} := \max\{Q(F(C), S) \mid C \in \mathcal{C}\}$ 
6  $C_{opt} :=$  one value of  $C$  where  $Q_{opt}$  is reached

```

Algorithm 4: Optimize cutoff C

For improvement in both complexity and controlling the quality of approximation it is desirable to replace this brute-force type algorithm for searching the optimum (Q_{opt}, C_{opt}) by more refined methods. In our applications, it turned out that the interpolation from \mathcal{C} to all of $[0, 1] \subset \mathbb{R}$ of the graph Γ_Q of the function $C \rightarrow Q(F(C), S)$ is rather good-natured as for finding global optima. In the vast majority of settings Γ_Q was a hill-formed curve, i.e. increasing (decreasing) to the left (right) of (C_{opt}, Q_{opt}) the top of which was the global maximum over all $[0, 1]$. See Figure 3 and Figure 4 for two typical Γ_Q examples.

3.4.5 Refined Method For Cutoff Selection

The brute-force method of Algorithm 4 has two disadvantages:

- Obtaining a good approximation of the global optimum takes many grid points to be evaluated which increases computation time.
- The quality of approximation is bound to the step-width of the grid.

Now we propose an algorithm which combines the advantage of the grid-based, fixed-step-width Algorithm 4—namely, independency of the starting point—with the advantages of flexible-step-width algorithms—improved speed and better control over the quality of approximation.

³Kappa is used for measuring agreement of two binary raters v and w here [3]. For binary raters, $\text{kappa}(v, w) = \frac{\text{accu}(v, w) - p_e}{1 - p_e}$ where $p_e = \frac{1}{n^2} (n_{v_i=0} \cdot n_{w_i=0} + n_{v_i=1} \cdot n_{w_i=1})$.

```

Input:  $B, D, T, p$  as in Algorithm 1.  $n_{steps} \in \mathbb{N}_{\geq 1}$ ,  $\varepsilon > 0$ 
1 Grid  $\mathcal{C} := \{t_1, \dots, t_{n_{steps}}\}$  equidistant in  $[0, 1]$ 
2 for  $C$  on  $\mathcal{C} \subset [0, 1]$  do
3   Compute  $F(C)$  by Algorithm 3
4   Compute  $Q(F(C), S)$ 
5 end
6  $Q_{opt,C} := \max\{Q(F(C), S) \mid C \in \mathcal{C}\}$ 
7  $C_{opt,C} :=$  one value of  $C$  where  $Q_{opt,C}$  is reached
8  $t_a := \max(0, C_{opt,C} - \frac{1}{2n_{steps}})$ 
9  $t_b := \min(1, C_{opt,C} + \frac{1}{2n_{steps}})$ 
10  $sw := \frac{t_b - t_a}{100}$  // step-width
11  $P_0 = (t_0, Q_0) := (t_a, Q(F(t_a), S))$ 
12  $P_1 = (t_1, Q_1) := (t_a + sw, Q(F(t_a + sw), S))$ 
13  $i := 1$ 
14 while true do
15   if  $|Q_i - Q_{i-1}| < \varepsilon$  then
16     break
17   end
18   if  $Q_i < 0$  then
19      $sw := |sw| \cdot 2$ 
20   end
21   if  $Q_i > 1$  then
22      $sw := -|sw| \cdot 2$ 
23   end
24   if  $Q_i \geq Q_{i-1}$  then
25      $sw := 1.5 \cdot sw$ 
26   end
27   if  $Q_i < Q_{i-1}$  then
28      $sw := -\frac{sw}{2}$ 
29   end
30    $P_{i+1} = (t_{i+1}, Q_{i+1}) := (t_i + sw, Q(F(t_i + sw), S))$ 
31    $i = i + 1$ 
32 end
33  $Q_{opt} := Q_i$ 
34  $C_{opt} := t_i$ 

```

Algorithm 5: Optimize cutoff C , refined method

In this algorithm we search for the optimum cutoff $C_{opt,C}$ on the points of a grid with fixed-step-width $\frac{1}{n_{steps}}$ first in order to get close to the global optimum. In the **while true** loop following we examine the interval $[t_a, t_b]$ of diameter $\frac{1}{n_{steps}}$ centered at $C_{opt,C}$ and initialize the—from now on—flexible step-width sw by,

say, $\frac{t_b - t_a}{100}$. Then we increase t by sw if the target function Q was non-decreasing when going from t_{i-1} to t_i . We step by $\frac{|sw|}{2}$ in the opposite direction if the target function Q was decreasing, supposing that we have overrun the peak of Q . We break if the most recent change of Q has not exceeded ε .

Using this algorithm we can dramatically reduce n_{steps} and thus save computation time spent for searching on the fixed-step-width grid \mathcal{C} because it suffices to get to $[t_a, t_b]$ containing the global optimum now and approximate further by iterating in the **while true** loop. Because searching on \mathcal{C} consists in a loop of completely independent evaluations of Q reducing n_{steps} to $\lfloor \frac{n_{steps}}{f} \rfloor$ improves computation time for searching on \mathcal{C} roughly by factor f .

3.5 Settings of Practical Applications

Let $B = \mathbb{Q}^n$, $B_i = \{x \in B \mid P_i(x) = 1\}$ where $P_i : B \rightarrow \mathbb{B}$ might be any Turing computable functions. The following types of function are prototypical examples of P_i . Let be $t > 0$ some constant.

$$P_i^e(x) = \begin{cases} 1, & x_i - t > 0 \\ 0, & \text{else} \end{cases}$$

We will call (i, x_i) with $P_i^e(x) = 1$ a *t-excess* henceforth.

$$P_i^a(x) = \begin{cases} 1, & |x_i| - t > 0 \\ 0, & \text{else} \end{cases}$$

We will call (i, x_i) with $P_i^a(x) = 1$ an *abs-t-excess* henceforth. Now let be $\underline{R}_i \leq \overline{R}_i$ numerical constants.

$$P_i^R(x) = \begin{cases} 1, & x_i < \underline{R}_i \quad \text{or} \quad x_i > \overline{R}_i \\ 0, & \text{else} \end{cases}$$

We will call (i, x_i) with $P_i^R(x) = 1$ a *ref-excess* henceforth. In practice, \underline{R}_i and \overline{R}_i might be the lower and upper edge, respectively, of a reference range.

Besides the above types of predicates P_i which are related directly to practical applications one can imagine more theoretical types of B_i (and thus P_i), e.g. linear half spaces ($L(x) > c$) or semi-algebraic sets ($p(x) > 0$).

3.6 Application 1: Identification of Positive Objects

Let us set $B = \mathbb{Q}^n$ and assume we are given a data set $D \subseteq B$ and a disjunctive subdivision $D = D^1 \cup D^0$ into positive and negative data points as in subsection 3.4. Set $T = D^1$ and $p = 100$. This means we are using the set of *all* positive data points as training set. In addition, we set cutoff $C = 1$.

With this special settings Algorithm 3 can be used as a means to identify positive data points. Setting $C = 1$ means that $F(x, T, C)$ as computed by Algorithm 3 predicts 1 (for “positive object”) if and only if $s(x, T) = 1$. $s(x, T) = 1$ if

and only if $\exists y \in T$ with $s(x, y) = 1$ by the very definition of $s(x, T)$ in subsection 3.2. By definition of $s(x, y)$ in subsection 3.2 this means

$$1 = \frac{\sum_{i=1}^s P_i(x) \cdot P_i(y)}{\sum_{i=1}^s P_i(x)}$$

or

$$\sum_{i=1}^s P_i(x) \cdot P_i(y) = \sum_{i=1}^s P_i(x)$$

which is equivalent to:

$$\forall i = 1, \dots, s : [P_i(x) = 1 \longrightarrow P_i(y) = 1]$$

So in this setting Algorithm 3 predicts an object x under test to be a positive object if there is at least one positive object y in $T = D^1$ such that all “excesses” (i, x_i) of x are “excesses” of y , too. If this is the case for the object under test x then we predict x to be a positive object and assign y to it.

3.6.1 Building and Solving a System of Implications

The method for object identification described above embodies a special case of Algorithm 3 by using the special settings of $T = D^1, p = 100, C = 1$. As an alternative one can take a different route to the same goal by first building a system of logical implications from all positive objects $y \in D^1$ (here $T = D^1$)

$$\exists y \in D^1 : \forall i = 1, \dots, s : (P_i(x) = 1 \longrightarrow P_i(y) = 1)$$

The implication system defined by the “excesses” of all $y \in D^1$ can be formulated as a Prolog program as well as the request whether a given object $x \in D$ is a positive one. The Prolog program finds those y satisfying the implication system by unification if there are any. We used **GNU Prolog** [1] for solving these implication systems. See [8] for an introduction to this topic.

At the end of this paragraph a Prolog program describing an implication system of the type mentioned above is listed. Each line starting with **defect(X) :-** is a rule which describes the thresholding of measurements of one positive object whereas the line **is_high(4, z)** formalizes the fact that measurement of parameter 4 of the object to be classified exceeded the threshold.

```

defect(X) :- is_high(16, X) , is_high(19, X) , is_high(21, X) ,
             is_high(22, X) ,      [...]      , is_high(380, X) ,
             is_high(383, X). % [Line 7]
defect(X) :- is_high(3, X) , is_high(13, X) , [...] ,
             is_high(385, X). % [Line 15]

%
% [...]
%
defect(X) :- is_high(5, X) , is_high(7, X) ,      [...]      ,
             is_high(375, X) , is_high(378, X) , is_high(381, X) ,
             is_high(384, X). % [Line 816]

is_high(4, z).
is_high(19, z).
is_high(26, z).
%
% [...]
%
is_high(319, z).
is_high(322, z).

```

3.7 Application 2: Predicting Positive Objects

In order to progress from object identification to predicting the positive/negative state of some object under test x yet unknown we do not try to find an object y of the training set whose set of “excesses” contains the set of “excesses” of the object under test but we are going to determine the degree of satisfiability by using the formula of subsection 3.2:

$$s(x, T) = \max_{y \in T} \frac{\sum_{i=1}^s P_i(x) \cdot P_i(y)}{\sum_{i=1}^s P_i(x)}$$

Unlike with object identification we use only a subset of positive objects T as training set. Note that—in the form we present here—we take only positive objects for training. Of course we can extend this algorithm to using a set of positive training objects T^1 and a set of negative training objects T^0 then predict an object under test x to be negative if $s(x, T^0) > C^0$ where C^0 is a second cutoff in addition to the cutoff $C^1 = C$ we use in Algorithm 3. Then we would need to extend Algorithm 4 to find an optimum pair of cutoffs (C_{opt}^1, C_{opt}^0) rather than finding just C_{opt} by replacing the one-dimensional base range or grid by a two-dimensional base range or grid, respectively.

In Figure 1 and Figure 2 we see plots showing $s(x, T)$ for 1000 and 10000 objects x where objects are represented by measurement vectors of chips from real-world chip fabrication. The training set size $|T|$ is 2% of all defective chips here. The chips have been reordered so that all defective chips appear on the left and all non-defective chips on the right. This is just for making the discrepancy of $s(x, T)$ for defective and non-defective chips x clearly visible. As can be seen, defective and non-defective chips are properly separated by their $s(x, T)$

Figure 1: Classifying 1000 chips with 2% training set size.

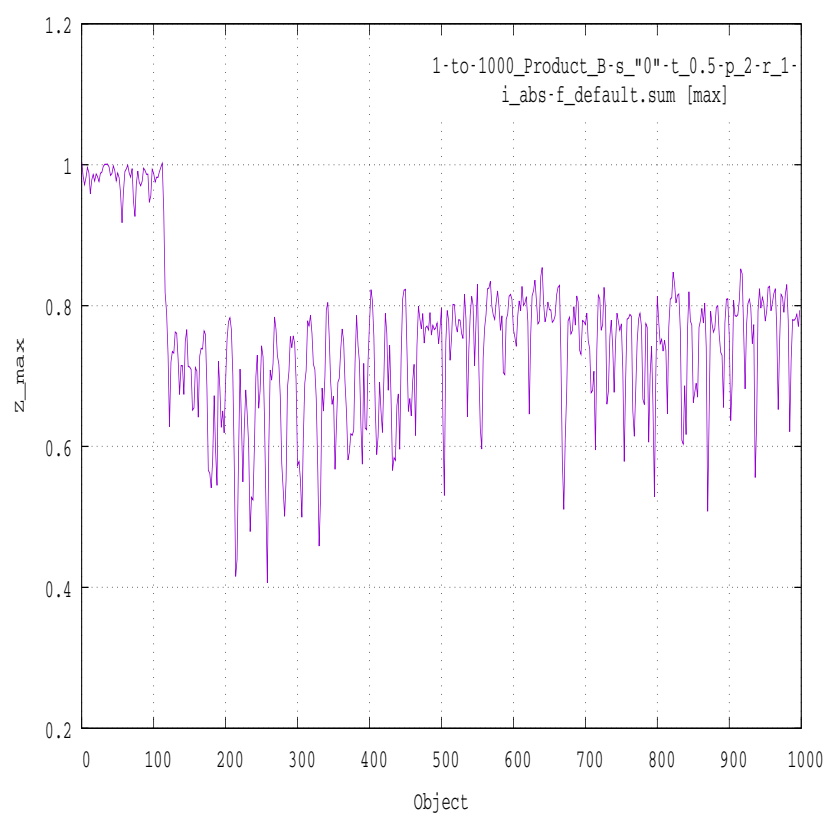


Figure 2: Classifying 10000 chips with 2% training set size.

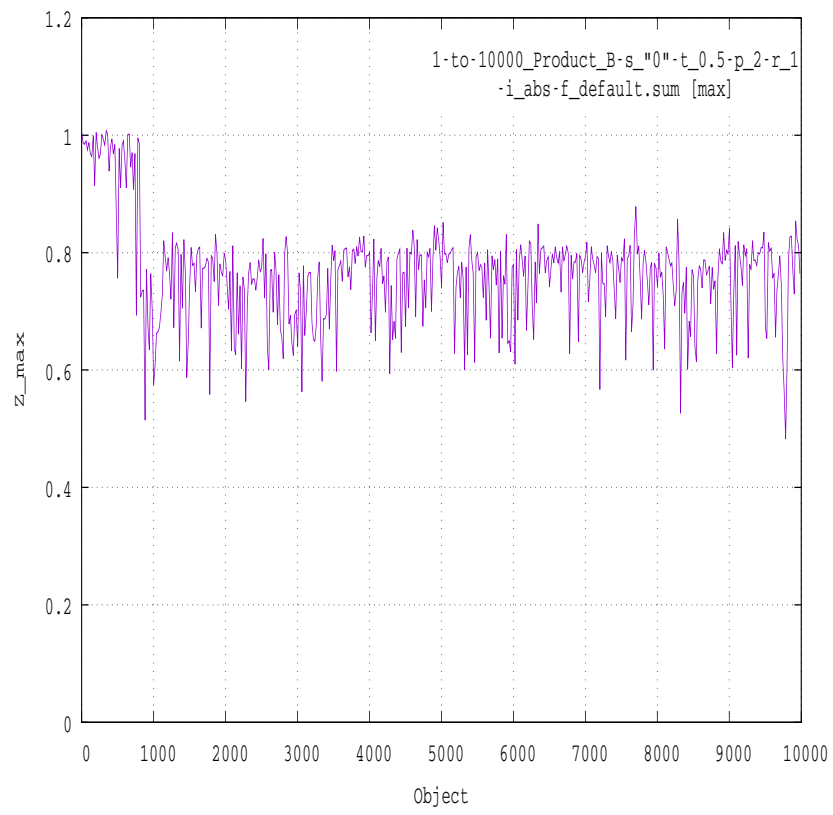
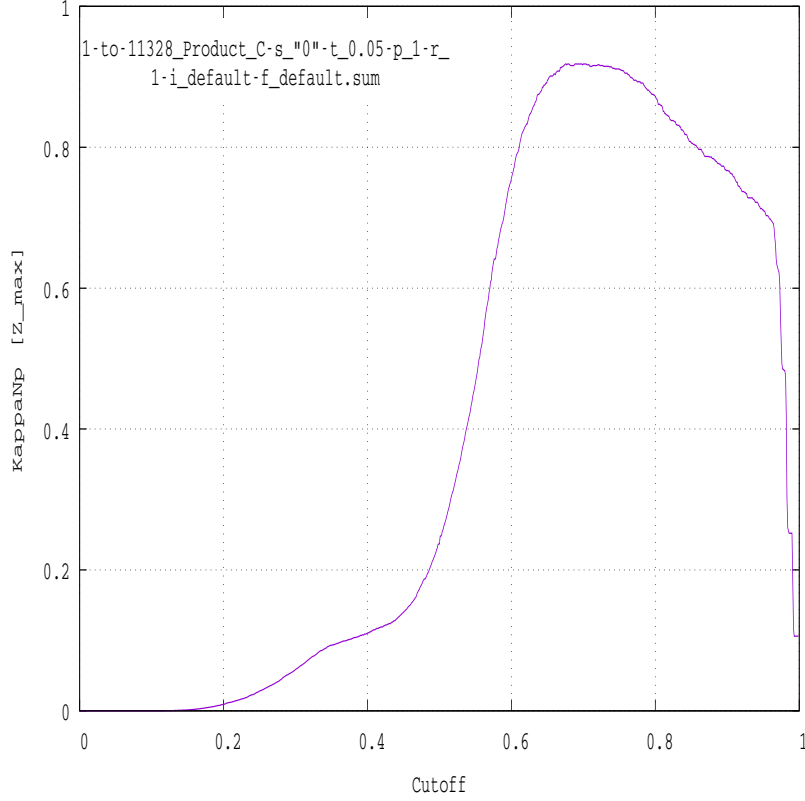


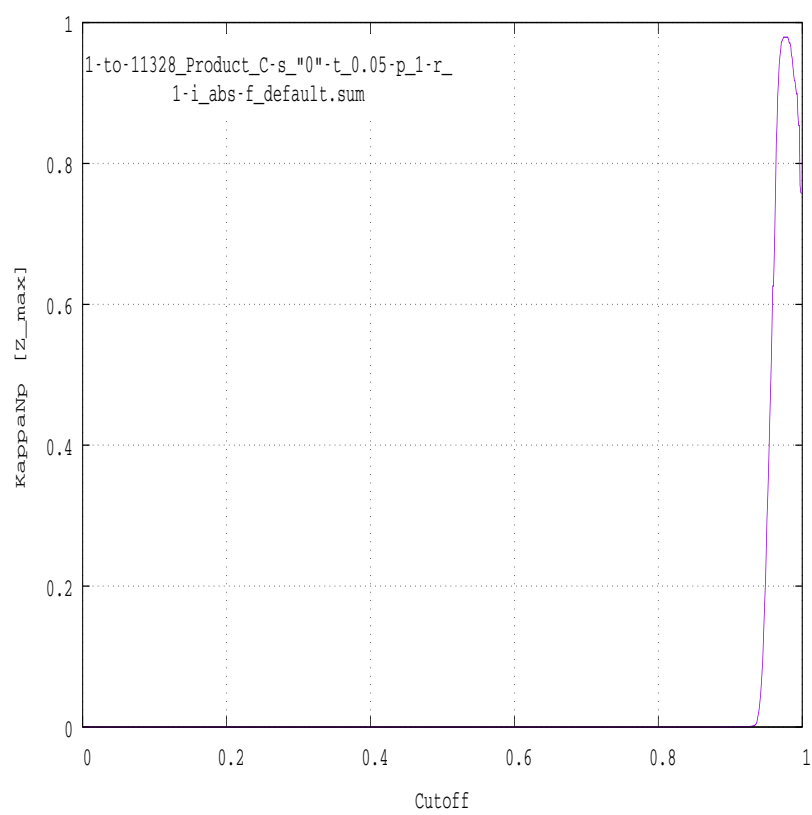
Figure 3: Kappa(cutoff) using t-excess thresholding.



values and this important property does not depend on the batch size—1000 or 10000—in this example.

Figure 3 and Figure 4 show two examples of how the kappa value of predictions changes when the cutoff varies from 0 to 1. This is what Algorithm 4 computes if we use Cohen’s kappa for $Q(v, w)$ and use in Algorithm 3 $s(x, T)$ as defined in subsection 3.2. We use an equidistant grid $\mathcal{C} \subseteq [0, 1]$ here. The first time we use thresholding by t-excess, the second time by abs-t-excess here. Both graphs have precisely one optimum (C_{opt}, Q_{opt}) whereby the hill of Figure 4 is sharper and higher than in Figure 3 which is rather typical with the type of data we used in our applications. Figure 3 and Figure 4 have been created by the same run with the same parameters as have been used in creating Figure 5 and Figure 6.

Figure 4: Kappa(cutoff) using abs-t-excess thresholding.



4 Experimental Setup

4.1 The Task

In short:

Given measurements and the defect states for chips of a small training set, predict the defect state of the remaining chips of the lot based on the measurements only.

So we are given measurement data from chip fabrication. The data is organized in so-called lots which is a set of wafers from production. Each wafer carries a fixed number of chips of the same product type. In what follows we abstract from wafers and consider a lot to be a set of m chips x^i of the same product type. Each chip x^i is represented by an n -vector of measurements (x_1^i, \dots, x_n^i) and its defect state $p(x^i) \in \mathbb{B}$. The meaning and ordering of these measurements is the same for all chips of some lot. The defect state is one bit per chip indicating whether the chip is to be considered OK or defective.

One general hypothesis our approach is based on is that defective devices can be predicted to some extent by looking at combinations of deviations from the respective component-wise means in measurement data.

Using the notation of subsection 3.4, let $D = \{x^1, \dots, x^m\}$ be the set of data points. A positive (negative) data point is a chip which is to be considered defective (non-defective) and D^1 (D^0) are the sets of defective (non-defective) chips, respectively.

The research question to be solved is: Find algorithms that are able to learn the function $f : \mathbb{R}^n \rightarrow \mathbb{B}$ which assigns the vector of measurements to the defect state of the respective chip:

$$(x_1, \dots, x_n) \mapsto p(x)$$

So, given (x_1^i, \dots, x_n^i) for a small set of training chips $x^i \in T \subseteq D^1$ we want an algorithm that predicts $p(x)$ for chips x of the same product type with defect state yet unknown, knowing only the measurement vector (x_1, \dots, x_n) of x . Note that we only need defect chips for training.

It is easy to see how to extend our algorithm to using non-defective chips for training, too. Using the notation of subsection 3.7, compute a second indicator

$$s_2(x, T_2) = \max_{y \in T_2} \frac{\sum_{i=1}^s (1 - P_i(x)) \cdot (1 - P_i(y))}{\sum_{i=1}^s (1 - P_i(x))}$$

where T_2 is a random subset consisting of negative objects (= non-defective chips). This indicator s_2 expresses maximum similarity of the object under test x to the objects in T_2 where the criterion shall be to *not* exceed the respective threshold now. Therefore we replace $P_i(x), P_i(y)$ of indicator s by $1 - P_i(x), 1 - P_i(y)$ in s_2 .

In our experiments we considered chips of 3 different product types A, B and C with the following properties:

| Product | #Chips | #Measurements/chip | continuous only |
|---------|--------|--------------------|-----------------|
| A | 8280 | 385 | yes |
| B | 11952 | 332 | yes |
| C | 11328 | 915 | no |

With product A and B we restricted measurement data to continuous parameters (currents, voltages etc.) whereas in product C we also used measurements of discrete parameters (e.g. counts, registers).

It is important that we do not use any meta-knowledge about the measurements. Neither do we know the types or units nor the meanings of the measurements. All we know is their numerical values and that (x_1, \dots, x_n) results from the same measurements in the same ordering for all chips x of some lot.

4.2 The Implementation

A program for Application 2 as described in subsection 3.7 has been realized in a combination of Python 3 (1296 lines) and Bash (112 lines). More recent versions of this program use the `Matplotlib` [7] and `Numpy` packages. A minimalist version has been implemented in only 31 lines (781 bytes) of Python 3 code. The “`for $x \in D \setminus T$` ”-loop has been parallelized by using the `multiprocessing` package and a speedup of ~ 3 could be achieved on a 4-core microprocessor.

A precursor for Application 1 as described in subsection 3.6 has been written in Awk, Bash and Prolog. This program was generating Prolog code for formalizing an implication system specified by the thresholding properties of the positive objects—see subsubsection 3.6.1—and was using Prolog’s unification algorithm for finding solutions.

5 Results

5.1 Properties

Algorithms 3 and 4 meet all of the five goals listed in section 2 and thus have properties which seem to make it well-suited for deriving the defect state of chips knowing measurement data.

As for the 5th goal—“reducing the number of tests”— we were successful even when limiting input data to continuous parameters while leaving out discrete parameters which may reduce the number of parameters from 900+ to 300-400. From these we could omit more parameters by limiting input data to the first measurement step and omit yet many more by applying our method of dimensional reduction as a preprocessing. More on these topics in subsections 5.3.4 and 5.3.5.

As for the 4th goal—“ability of coping with large amount of data”— we expect it to be possible to handle even much larger lots of data facing the favorable runtime behaviour of our algorithm.

The hardware demands of all algorithms presented in this paper are low. The speed of classifications performed for generating all data mentioned in this paper ranged from 8738 objects/sec to 415 objects/sec on a Pentium i5-750 (4 × 2.67 GHz) with a mean of 3068 objects/sec (3rd and 4th goal).

5.2 Free Parameters

Using Algorithms 3 and 4 we had three free parameters:

- p (= percentage of training set T from all positive objects)
- seed (for randomly selecting T)
- threshold t

The meaning of t is explained in subsection 3.5. We were using sets B_i defined by the thresholding functions $P_i^e(\cdot)$ (t -excess) and $P_i^a(\cdot)$ (abs- t -excess) described there.

The value of t influences the quality of prediction to some extent but it turned out that one can get good results even with a default $t = 0.5$. We were setting seed=1 mostly. In our experiments we were testing a wide range of p from 1 to 50. Note that—unlike with other algorithms— p refers to a percentage of the positive objects only. If, for example, 10% of all chips in a lot are defective and we set $p = 2$ then Algorithm 1 takes only 0.2% (not 2%) of all chips for training, all of which are defective. Since defective chips were a small minority in a lot our training sets were frequently much smaller than with other algorithms applying the “10:90”- or “20:80”-rule in determining the training set size.

In the following tables we will be writing z_{\max} and z_{\min} for two types of coincidence index, namely z_{\max} for $s(x, T) = \max\{s(x, y) \mid y \in T\}$ and z_{\min} for $s(x, T) = \min\{s(x, y) \mid y \in T\}$ using notations of “**Task:**” in subsection 3.2.

5.3 Results for Application 2

The first problem we set out to solve⁴ was to predict the defect state of chips knowing only a set of measurements as is described by Application 2 in subsection 3.7.

| Product | #Chips classified | Train set | t | Coinc. index | Thresholding | Accuracy | Kappa |
|---------|-------------------|-----------|------|--------------|--------------|----------|-------|
| A | 5000 | 35% | 0.48 | z_{\max} | t-excess | 0.943 | 0.484 |
| A | 5000 | 35% | 0.94 | z_{\max} | abs-t-excess | 0.954 | 0.633 |
| B | 5000 | 2% | 0.5 | z_{\max} | t-excess | 0.967 | 0.788 |
| B | 5000 | 2% | 0.5 | z_{\max} | abs-t-excess | 0.990 | 0.938 |
| B | 10000 | 15% | 0.5 | z_{\max} | t-excess | 0.979 | 0.824 |
| B | 10000 | 1% | 0.5 | z_{\max} | abs-t-excess | 0.990 | 0.929 |
| C | 11328 | 1% | 0.05 | z_{\max} | t-excess | 0.992 | 0.918 |
| C | 11328 | 1% | 0.05 | z_{\max} | abs-t-excess | 0.998 | 0.979 |

As can be seen, thresholding by 1 iff $|x_i| > t$ (abs-t-excess in the above table, $P_i^a(x)$ in subsection 3.5) typically leads to better results than just $x_i > t$ (t-excess, $P_i^e(x)$). This is not surprising because the latter does not catch conditions $x_i < -t$ (i.e. measurements being notably lower than the mean value) whereas the former does.

The next two plots—Figure 5 and Figure 6—show z_{\max} at classifying a complete lot of 11328 chips of product C in one run with the aforementioned two different thresholding functions t-excess ($x_i > t$) and abs-t-excess ($|x_i| > t$).

Both plots show how easy it is to place a horizontal cutoff line in order to cleanly separate the defective chips from the non-defective chips by the discrepancies of their z_{\max} values. As the corresponding two lines in the first table in section 5.3 show, abs-t-excess is slightly superior to t-excess here with a kappa value of 0.979 vs. 0.918.⁵

Figure 7 is an example of how kappa and the quotient of averages

$$Q_{\text{avg}, z_{\max}} = \frac{\text{avg } z_{\max}(\text{defective chips})}{\text{avg } z_{\max}(\text{non-defective chips})}$$

depend on threshold t . The data stems from classifying 10000 chips of product B in one run with 2% training set size using abs-t-excess thresholding with threshold t varying from 0.1 to 1. Even though intuition tells that higher $Q_{\text{avg}, z_{\max}}$ values tend to be associated with higher kappa values there is not a direct relation of high $Q_{\text{avg}, z_{\max}}$ values and high kappa. One reason for this lies in the fact that in order to find a good z_{\max} cutoff for separating defective chips from

⁴Actually the very first problem was identification of defective chips—described by Application 1 in subsection 3.6—the promising results of which were encouragement for us to tackle the problem baselying to Application 2.

⁵Both plots look like it were easily possible to find a cutoff value which would separate the defective chips from the rest with an accuracy of 100% and kappa value of 1.0. In truth there are some few peaks in these graphs of z_{\max} which are fine enough for being invisible in lack of unlimited rendering resolution but which push down both accuracy and kappa slightly below the optimum of 1.0.

Figure 5: z_{\max} using t-excess for thresholding.

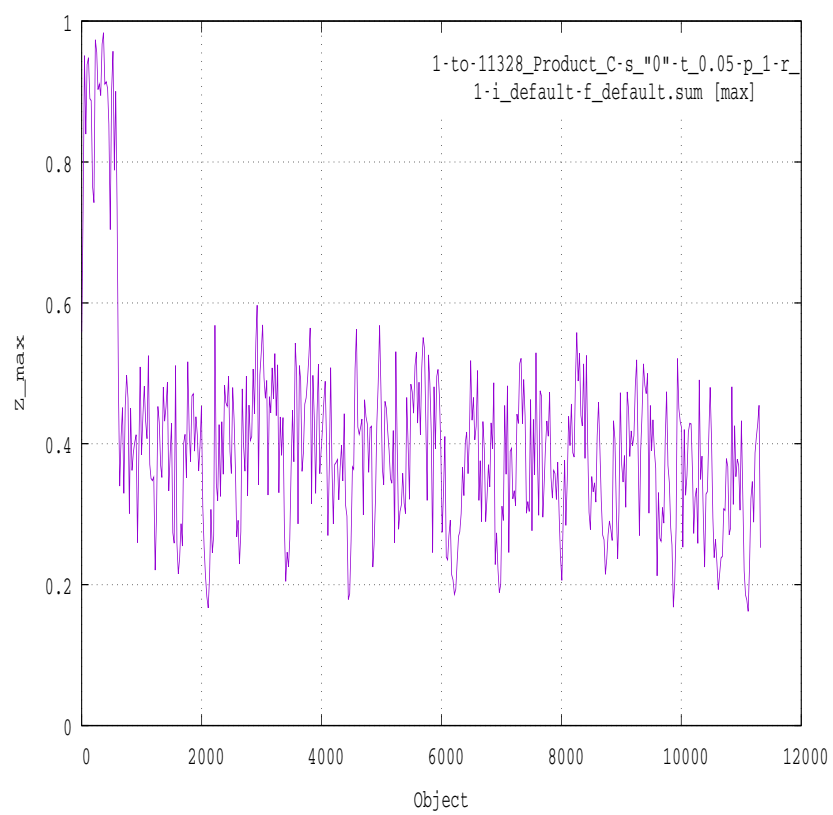


Figure 6: z_{\max} using abs-t-excess for thresholding.

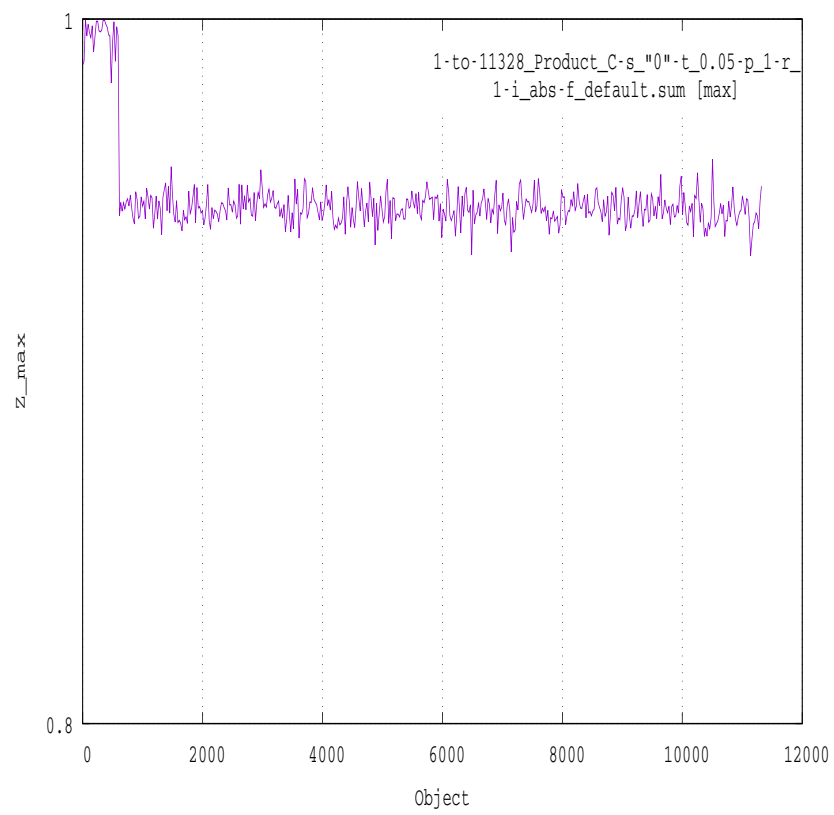
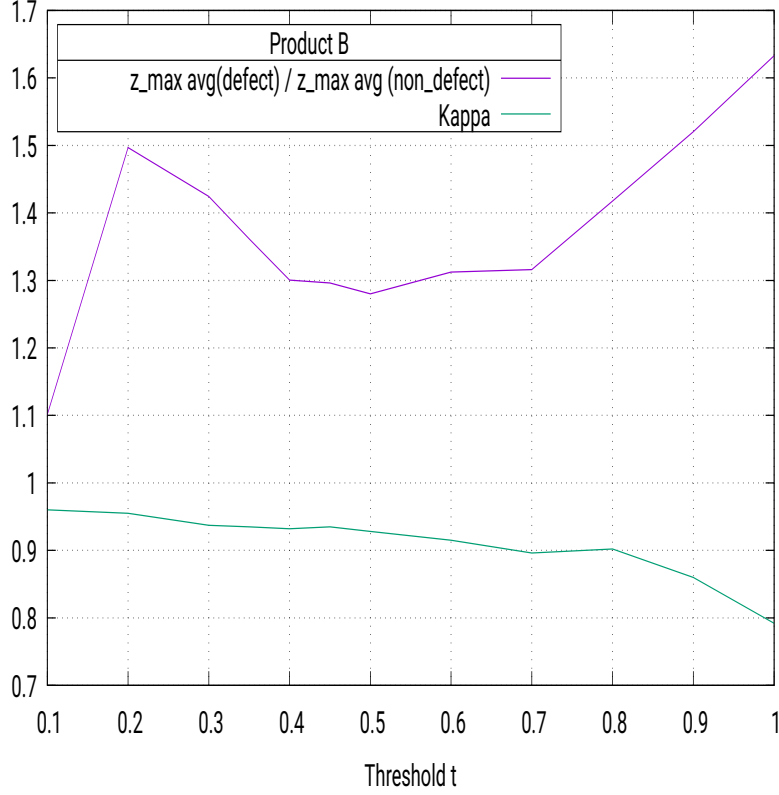
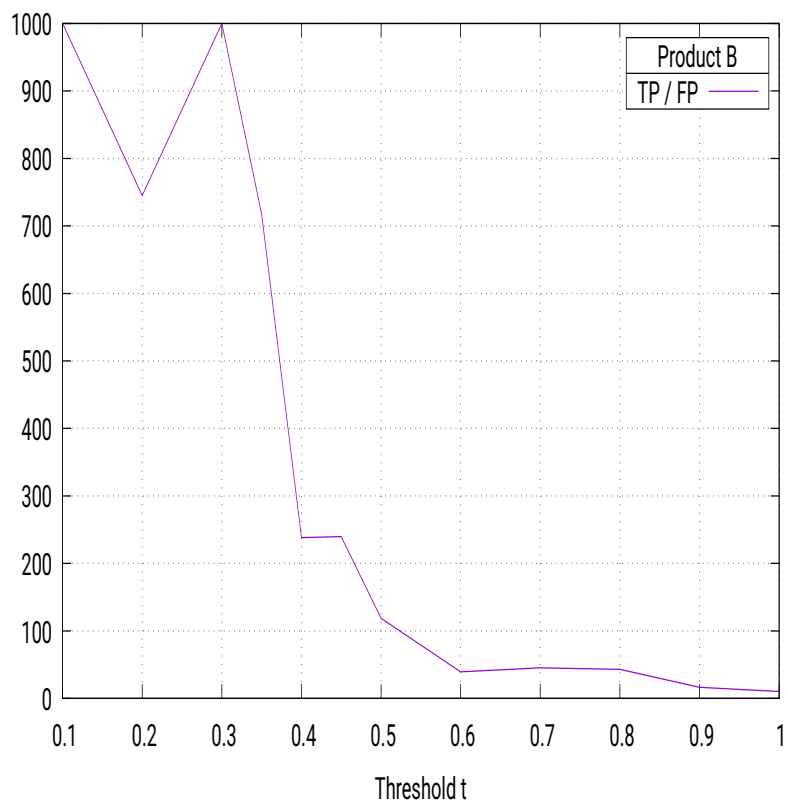


Figure 7: Quotient of z_{\max} averages and kappa.



non-defective ones other properties like variance and regularity/roughness of the z_{\max} graph—see Figure 5 and Figure 6—play important roles. Figure 7 also shows the excellent kappa levels—0.96 in this setting—that can be reached by our algorithms and the relative independence of kappa from threshold t here: $\text{kappa} > 0.78$ irregardless of the choice of $t \in [0, 1]$. Figure 8 stems from the same data and parameters as Figure 7 and shows an example of how the true-positive-false-positive quotient depends on threshold t . A high $\frac{TP}{FP}$ value is an important performance criterion of methods for defect prediction in semiconductor fabrication because high $\frac{TP}{FP}$ values directly translate into reducing costs by avoiding to scrap non-defective devices based on false predictions. As Figure 8 shows, by applying our algorithmic method we risk scrapping only one functioning device per 1000 defective devices predicted correctly which is an excellent performance facing that minimum demands may be as low as 2.

Figure 8: $\frac{TP}{FP}$ over threshold t .



5.3.1 Predicting Specific Types of Failure

In quality control of chip fabrication it is informative to know not only that a chip will be defective—and thus should not be bonded, boxed and shipped—but also the specific type of defect. Defective chips can be classified by assigning those chips to the same soft bin (SBIN) which suffer from the same type of defect.

Predicting whether the type of defect of some chip under test belongs to a certain SBIN S can be formulated as a variant of the aforementioned problem of predicting the defect state of chips. For doing this, we just substitute the target function $p : D \rightarrow \mathbb{B}$ we used for defect state prediction,

$$p(x) = 1 \text{ iff data point } x \text{ belongs to a defective chip,}$$

by:

$$p(x) = 1 \text{ iff data point } x \text{ is assigned to } S.$$

| Pro- duct | SBIN | Chips classi- fied | Train set | t | Coinc. index | Thre- sholding | Accu- racy | Kappa |
|--------------|------|--------------------------|--------------|------|-----------------|-------------------|---------------|-------|
| B | "6" | 11952 | 30% | 0.05 | z_{\max} | t-excess | 0.999 | 0.749 |
| B | "7" | 11952 | 50% | 0.05 | z_{\min} | t-excess | 1.000 | 0.895 |

We have chosen SBINs "6" and "7" because these two were the SBINs most frequently occurring in the baselying data material. Though there were very few chips with these defect types—only 50 and 40 out of 11952 chips, which is 4.2‰ and 3.3‰, respectively. So even in these two cases there were very few positive objects to be used for training. Because it is not possible to learn if the sample frequency is too low we suspect that if we had more samples of defective chips with a specific defect type for disposal then other SBINs could be predicted, too.

5.3.2 Detecting Iris Type

In order to know whether our algorithm can learn functions from an application range different than detecting chip defects we applied it to the classic iris flower data set [5] in the corrected form of [4] (samples #35 and #38).

| Iris type | Train set | t | Coinc. index | Thre- sholding | Accu- racy | Kappa |
|--------------|--------------|-----|-----------------|-------------------|---------------|-------|
| setosa | 20% | 0.1 | z_{\max} | t-excess | 0.971 | 0.928 |
| versicolor | 30% | 1.0 | z_{\max} | abs-t-excess | 0.852 | 0.557 |
| virginica | 30% | 0.9 | z_{\max} | t-excess | 0.919 | 0.797 |

As one can see, setosa and virginica can be detected quite successfully whereas detecting versicolor seems harder to our algorithm. This is in accordance with the—both expected and observed—strengths of our algorithm: Looking at visualizations of the iris flower data set one sees that sepal and petal length and

width, resp., of the versicolor species are in a medium range whereas sepal and petal length and width, resp., of setosa and virginica are on the lower and upper ends of the value ranges. Since our algorithms are made for identifying and detecting defective chips—where certain combinations of exceedingly low or exceedingly high values frequently indicate a defective chip—it is no surprise that detecting setosa and virginica is rather easy to our algorithm whereas detecting versicolor is harder.

5.3.3 Prototypical Positive Objects

In order to gain insights into why defective chips can be detected by looking for maximum similarity regarding $s(x, T)$ —see subsection 3.7—we created histograms for answering the following questions:

Given: chip $y \in T$

Question: how big is $|\{x \in D^1 \mid s(x, y) = s(x, T)\}|$?

We will call the latter number $n(y)$ and define

$$H(y) := \frac{n(y)}{|D^1 \setminus T|}$$

In words, $H(y)$ is the amount of those defective chips which have maximum similarity to $y \in T$ in all defective chips outside the training set. Remember that we only classify chips outside the training set T because we do not consider classifying chips of the training set an interesting goal in Application 2.

An interesting observation in most of our experiments was that in most settings $H(y)$ was relatively large for a small number of chips $y \in T$ with a steep decrease towards those $y \in T$ with smaller $H(y)$.

Example of a full histogram (product B, 5000 chips to be classified, 13% training set):

| y (= Train object ID) | $H(y)$ % | $n(y)$ (#chips) |
|----------------------------|-------------|--------------------|
| 3762 | 54.39 | 223 |
| 8407 | 8.54 | 35 |
| 8342 | 8.29 | 34 |
| 14361 | 5.85 | 24 |
| 3461 | 3.66 | 15 |
| 7185 | 3.41 | 14 |
| 51 | 3.41 | 14 |
| 33 | 2.93 | 12 |
| 9650 | 2.20 | 9 |
| 2875 | 2.20 | 9 |
| 4856 | 0.98 | 4 |
| 7007 | 0.98 | 4 |
| 159 | 0.73 | 3 |
| 11586 | 0.49 | 2 |
| 3693 | 0.49 | 2 |
| 1168 | 0.49 | 2 |
| 6927 | 0.49 | 2 |
| 307 | 0.24 | 1 |
| 7963 | 0.24 | 1 |

As can be seen easily, almost all defective chips outside the training set are most similar—regarding $s(x, T)$, see subsection 3.7—to only a small subset of the training samples. In this example, $\sim 95\%$ of all defective chips (410 in this example) are most similar to only 10 training samples, namely the 10 topmost chips in the table above. Chips who occur near the top of such a histogram possess specific properties that allow for detecting a multitude of defective chips. We call these chips *prototypical defective chips*.

In the following table we show $n(y)$ and $H(y)$ for the topmost 3 training chips $y_1, y_2, y_3 \in T$ of the respective histogram. The parameters belonging to the lines of this table are the same as in the first table of subsection 5.3.

| Pro- duct | #Chips classified | Train set | Thre- sholding | Accu- racy | Kappa |
|--------------|----------------------|--------------|-------------------|---------------|-------|
| A | 5000 | 35% | t | 0.943 | 0.484 |
| A | 5000 | 35% | abs-t | 0.954 | 0.633 |
| B | 5000 | 2% | t | 0.967 | 0.788 |
| B | 5000 | 2% | abs-t | 0.990 | 0.938 |
| B | 10000 | 15% | t | 0.979 | 0.824 |
| B | 10000 | 1% | abs-t | 0.990 | 0.929 |
| C | 11328 | 1% | t | 0.992 | 0.918 |
| C | 11328 | 1% | abs-t | 0.998 | 0.979 |

| Pro- duct | #Chips classified | Train set | Thr. | $H(y_1)\%$ $(n(y_1))$ | $H(y_2)\%$ $(n(y_2))$ | $H(y_3)\%$ $(n(y_3))$ |
|--------------|----------------------|--------------|-------|--------------------------|--------------------------|--------------------------|
| A | 5000 | 35% | t | 3% (12) | 3% (12) | 3% (12) |
| A | 5000 | 35% | abs-t | 11% (38) | 5% (18) | 5% (18) |
| B | 5000 | 2% | t | 27% (126) | 17% (80) | 13% (59) |
| B | 5000 | 2% | abs-t | 33% (151) | 32% (147) | 16% (72) |
| B | 10000 | 15% | t | 21% (146) | 7% (47) | 5% (35) |
| B | 10000 | 1% | abs-t | 40% (322) | 38% (308) | 15% (122) |
| C | 11328 | 1% | t | 34% (204) | 28% (171) | 19% (116) |
| C | 11328 | 1% | abs-t | 38% (230) | 37% (223) | 12% (71) |

(Thr. = Thresholding)

As in the full histogram example, we see that most of the defective chips to be classified have maximum similarity to only a small set of $y \in T$. It may be worthwhile to investigate properties of prototypical defective chips more in-depth for they seem to embody a kind of “blueprint” for whole classes of defective chips. So modifying fabrication with the goal of avoiding prototypical defective chips might eliminate whole classes of defective devices.

This observation also held true when applying our algorithm to the iris flower classification problem. In these histograms we found one sample y with $H(y) = 90\%$, $H(y) \sim 49\%$ and $H(y) \sim 91\%$ when attempting to detect setosa, versicolor and virginica, resp.

Returning to chip measurement data—as can be seen from the above table, accuracy and kappa are worse with product A than with products B and C and the steepness of $H(y)$ for product A is low if compared to products B and C. Whether those chip measurement data sets which are generally easier to our algorithm are associated with higher Gini coefficients of $H(y)$ may be subject of further research.⁶ The following table shows the confusion matrices belonging to the lines of the first table of subsection 5.3.

| Pro- duct | Accu- racy | Kappa | TP | FP | TN | FN | $\frac{TP}{FP}$ |
|--------------|---------------|-------|-----|----|-------|-----|-----------------|
| A | 0.943 | 0.484 | 118 | 34 | 4418 | 241 | 3.5 |
| A | 0.954 | 0.633 | 153 | 17 | 4435 | 206 | 9.0 |
| B | 0.967 | 0.788 | 331 | 34 | 4499 | 131 | 9.7 |
| B | 0.990 | 0.938 | 417 | 5 | 4528 | 45 | 83.4 |
| B | 0.979 | 0.824 | 535 | 47 | 9129 | 164 | 11.4 |
| B | 0.990 | 0.929 | 719 | 4 | 9172 | 97 | 179.8 |
| C | 0.992 | 0.918 | 524 | 4 | 10709 | 84 | 131.0 |
| C | 0.998 | 0.979 | 584 | 0 | 10713 | 24 | ∞ |

Facing that a minimum requirement for considering a defect chip detection method to be feasible might be $\frac{TP}{FP} > 1$ —that is, allowing for scrapping at

⁶The Gini coefficient G measures a degree of inequality in a distribution [6]. If y_1, \dots, y_n are non-negative values of n objects then $G = \frac{\sum_{i=1}^n \sum_{j=1}^n |y_i - y_j|}{2n \cdot \sum_{i=1}^n y_i} \in [0, 1]$.

most one intact chip for every defective chip being properly detected in the long run—the confusion matrices in the above table are very good to excellent. It is even possible to reach $FP = 0$ which implies $\frac{TP}{FP} = \infty$ with product C.

5.3.4 Predicting Defect States Knowing Only Part of Measurement Data

In this subsection we describe our solution to a set of important problems circling around saving costs by omitting measurements while computing still accurate and meaningful predictions. Differing relevant measurements from those which are irrelevant for keeping a certain quality level and thus can be omitted is generally a problem of high importance in fabrication and quality assurance. On the one side measurements in fabrication are costly and take time so it is desirable to reduce the amount of measurements carried out to a minimum. On the other side sophisticated measurements enable detecting defects early and the earlier they are detected the better and—mostly—the cheaper. In addition, the time and space complexity of typical classification algorithms depends at least linearly on the number of features which may be an extra motivation for example in environments with real-time demands.

The measurement data we had at our disposal consisted in parameter packs—so-called measurement steps—carrying names like T1, T2, Y5. Each measurement belongs to a certain measurement step. Measurements of different measurement steps differ in the step of fabrication they were taken at and their type. So T1 measurements are carried out in a measurement step of a fabrication step earlier than T2 measurements.

To be more specific, the problem we turn to now can be formulated like this.

Is it possible to predict the defect state that would appear after measurement step T2 if all we know is measurement data of measurement step T1?

This problem is harder: The classifier has to predict the T2 defect state without knowing any T2 measurements.

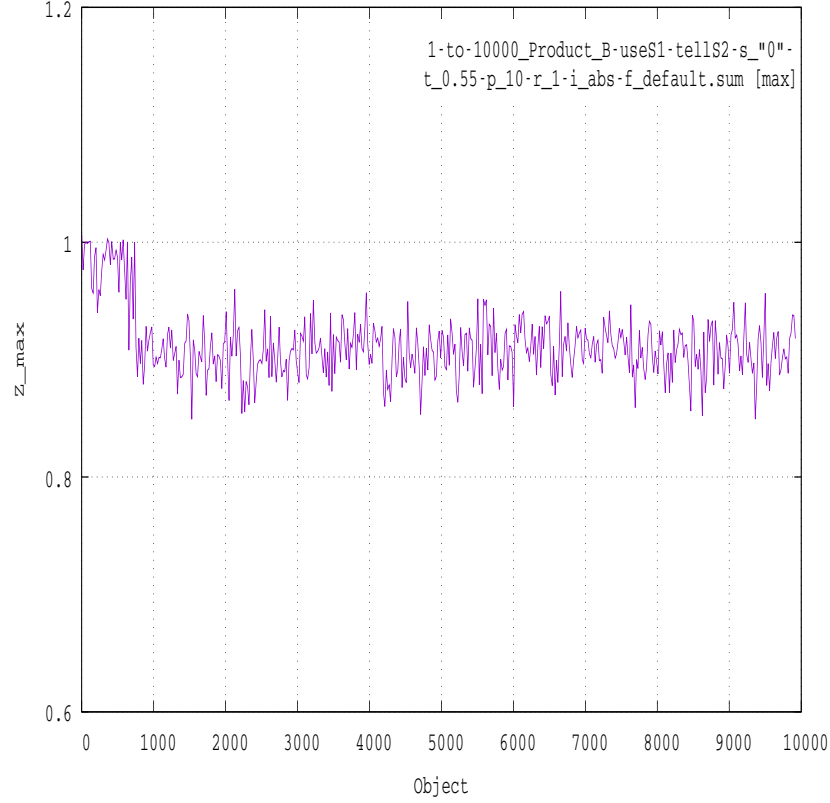
So in case of product B the first 77 (T1) of 332 (T1+T2) measurements per chip are given as input to the classification algorithm, and in case of product C, only the first 429 (T1) of 915 (T1+T2) measurements per chip are given.

Our results show that our algorithmic methods are a means to solve this harder problem, too, with good to very good kappa values and excellent accuracy.

| Product | #Chips classified | Train set | t | Coinc. index | Thresholding | Accuracy | Kappa |
|---------|-------------------|-----------|------|--------------|--------------|----------|-------|
| B | 10000 | 10% | 0.55 | z_{\max} | abs-t-excess | 0.970 | 0.772 |
| B | | | | z_{\min} | | 0.968 | 0.713 |
| C | 11328 | 1% | 0.05 | z_{\max} | | 0.979 | 0.760 |
| C | | | | z_{\min} | | 0.989 | 0.885 |

Figure 9 and Figure 11 show how z_{\max} or z_{\min} —as computed by Algorithm 3—can be used to classify in one run the T2 defect state of 10000 and 11328

Figure 9: z_{\max} predicting T2 defect state knowing only T1 measurements.



chips knowing only T1 measurements. Figure 10 and Figure 12 display the graph Γ_Q belonging to Figure 9 and Figure 11.

Prototypical defective chips. In the following two tables we list the top lines of histograms counting for each training chip $y \in T$ how many defective chips $x \in D^1 \setminus T$ to be classified have maximum $s(x, t)$ for $t = y$. See 5.3.3 for definitions of $n(y)$ and $H(y)$.

Top of histograms for product B (left table) and product C (right table):

Figure 10: Kappa(cutoff) of the foregoing figure.

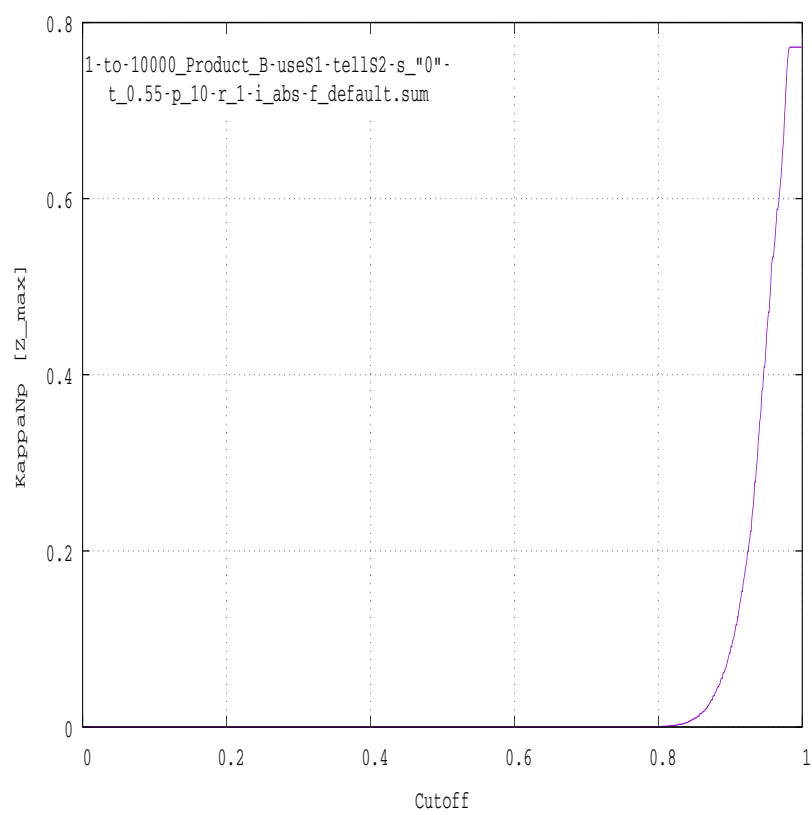


Figure 11: z_{\min} predicting T2 defect state knowing only T1 measurements.

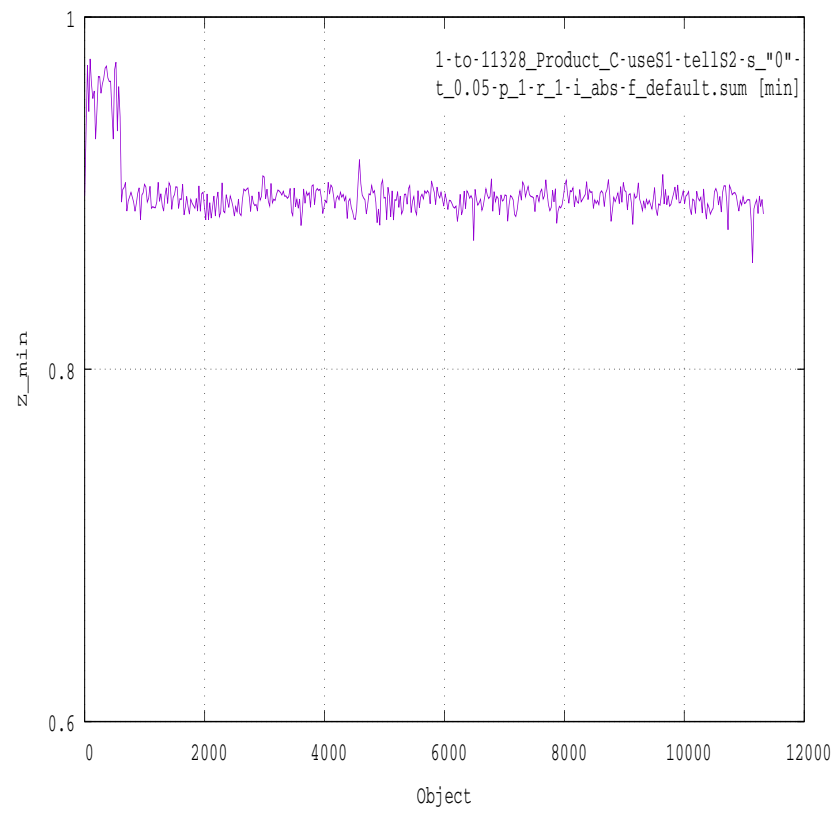
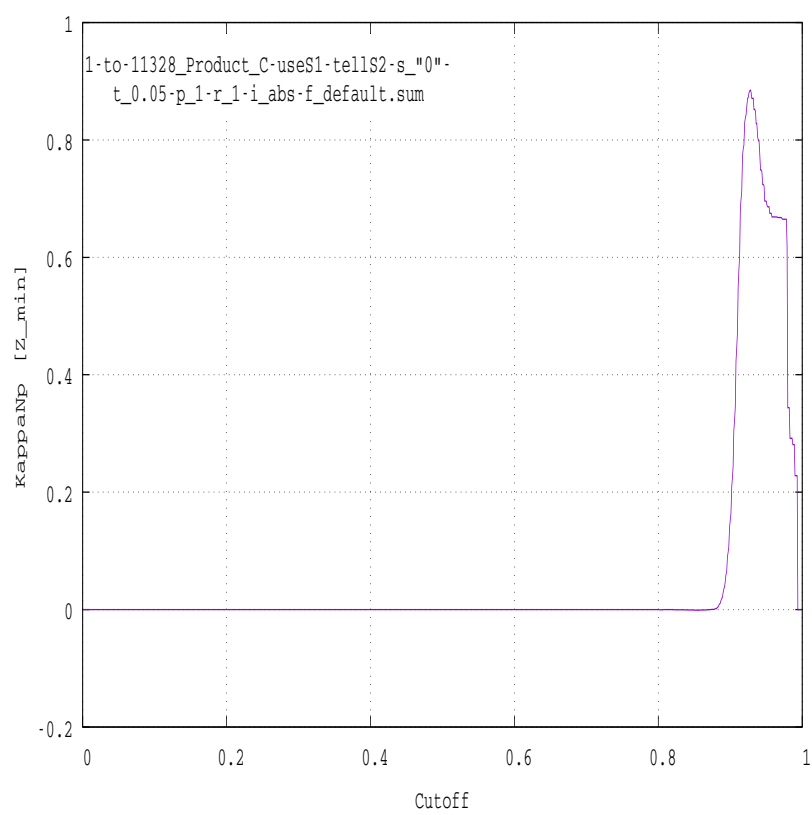


Figure 12: Kappa(cutoff) of the foregoing figure.



| y (= Train object ID) | $H(y)$ % | $n(y)$ (#chips) |
|----------------------------|-------------|--------------------|
| 148 | 23.69 | 176 |
| 7032 | 18.44 | 137 |
| 38 | 16.02 | 119 |
| 195 | 7.00 | 52 |
| 1019 | 5.11 | 38 |
| 6365 | 4.98 | 37 |
| 10020 | 4.85 | 36 |
| 60 | 3.36 | 25 |
| 8526 | 3.36 | 25 |
| 2504 | 2.69 | 20 |
| 9984 | 2.15 | 16 |
| 11464 | 1.88 | 14 |
| 1718 | 1.75 | 13 |
| 977 | 1.35 | 10 |

| y (= Train object ID) | $H(y)$ % | $n(y)$ (#chips) |
|----------------------------|-------------|--------------------|
| 235 | 37.50 | 228 |
| 10392 | 36.68 | 223 |
| 6030 | 11.68 | 71 |
| 9193 | 10.20 | 62 |
| 6194 | 3.62 | 22 |

For both products we see again the phenomenon of prototypical defective chips described in 5.3.3: Relatively few chips y have maximum $s(x, y)$ with the vast majority of defective chips.

An easier variant. A variant of minor practical importance is the task of learning the T1 defect state knowing T1 and T2 measurements. We have tackled this task using our algorithms and could reach an accuracy of 100.0% and kappa 0.997 with only 2 out of 10000 chips having been classified wrongly at classifying 10000 chips of product B using z_{max} , 40% training set, threshold 0.04. When using z_{min} results are only slightly worse with accuracy 99.7% and kappa 0.961.

5.3.5 Dimensional Reduction

As explained in subsection 5.3.4, reducing the number of measurements without experiencing an intolerable reduction in failure detection quality is a worthwhile task. In subsection 5.3.4 we investigated how all measurements of a complete measurement step can be omitted.

To go further we developed a method for reducing the number of measurements by omitting features with specific properties as a preprocessing step. This method has one free parameter we call *sharpness* by which we can tune the amount of reduction.

The algorithm. The set of input data points D must be given as lines of a $m \times n$ -matrix, auto-scaled by column. Algorithm 2 can be used for this. In what follows we use “ \sqcup ” as denotation for disjunctive decomposition of a set. $\{1, \dots, m\} = I^0 \sqcup I^1$ is the index decomposition induced by splitting D into negative and positive objects, $D = D^0 \sqcup D^1$.

```

Input:  $D = \{x_1, \dots, x_m\} \subseteq \mathbb{R}^n$  ( $m$  line vectors) auto-scaled by column,
          $\{1, \dots, m\} = I^0 \sqcup I^1$ 
Input: sharpness  $\in \mathbb{N}_{\geq 0}$ 
Output:  $E \in \mathbb{R}^{m \times n^*}$ ,  $n^*$ 
1 for  $i \in I^1$  do
2    $m := \max\{|x_{ij}| : j \in \{1, \dots, n\}\}$ 
3    $\text{MaxIndices}_i := \{j \in \{1, \dots, n\} : |x_{ij}| = m\}$ 
4 end
5 for  $j = 1 \dots n$  do
6    $\text{NumOccu}_j := \sum_{\substack{i=1, \dots, m \\ i \in I^1}} |\text{MaxIndices}_i \cap \{j\}|$ 
   // count how many positive objects  $x_i \in I^1$  have maximum
   // absolute value in the  $j$ -th component of the auto-scaled data
7 end
8  $k := 0$ 
9 for  $j = 1 \dots n$  do
10  if  $|\text{NumOccu}_j| \geq \text{sharpness}$  then
11     $k := k + 1$ 
12    for  $i = 1 \dots m$  do
13       $e_{i,k} := x_{i,j}$ 
14    end
    // copy column  $j$  from  $D$  to  $E$ 
15  end
16 end
17  $n^* := k$ 

```

Algorithm 6: dim-reduce(D , sharpness)

Time complexity is linear in the size $m \times n$ of the input matrix if we neglect polylogarithmic factors.

The following table shows some results of classifying 11328 chips of product C in one run with parameters known from further above: 1% training set size, abs-t-excess thresholding, goal: predicting defect state of measurement step T2 knowing only measurements of T1. The number of features before reduction is 429 (= total number of measurements per chip in T1) whereas the number of features after dimensional reduction is shown under #feat. omitted. Sharpness 0 in the first line of the table means no dimensional reduction i.e. all 429 features are given to the classification algorithm.

| Sharpness of reduct. | #feat. omitted | %feat. omitted | Accuracy [z_{min}] | Kappa [z_{min}] | $\frac{TP}{FP}$ |
|-------------------------|-------------------|-------------------|---------------------------|------------------------|-----------------|
| 0 | 0 | 0% | 0.989 | 0.885 | 33.3 |
| 1 | 283 | 66.0% | 0.974 | 0.664 | $+\infty$ |
| 2 | 346 | 80.7% | 0.973 | 0.656 | 34.4 |
| 3 | 379 | 88.3% | 0.946 | 0.194 | 0.234 |
| 4 | 387 | 90.2% | 0.946 | 0.188 | 0.201 |

Interpretation: By performing our dimension reduction with sharpness 1 we can omit 66% of measurements and still predict T2 defect state with accuracy 97.4%, kappa 0.664. With sharpness 2 we can omit 80.7% of measurements and reach accuracy 97.3%, kappa 0.656 which is only marginally worse. With sharpness ≥ 3 the quality of prediction—clearly visible by looking at kappa and $\frac{TP}{FP}$ —declines rapidly so that the recommendation would be to not go farther than sharpness = 2 and thus save 80.7% of measurements.

The important true-positive-false-positive quotients are impressively high when using sharpness < 3 .

6 Conclusion

We have presented a fast generic algorithm and a method for dimensional reduction for detecting abnormal objects in high-dimensional data which has been applied to data from wafer fabrication in order to predict defect states of tens of thousands of chips of several products based on measurements or part of measurements successfully.

When compared with the optimization principle of typical neural-net based algorithms, we are looking for the optimal rater of a very limited set of possible raters—given by the constants computed in the training step and the structural simplicity of the operations graph and flow-chart of our algorithms with only one or two undetermined variables to optimize over—instead of looking for the optimal rater in a high-dimensional set of possible raters with many undetermined variables to optimize over.

The question whether these methods can be applied in situations where the connections of measurement data and defect state are of a more indirect nature like when trying to predict backend defects knowing frontend measurement data is subject of ongoing research.

List of Figures

| | | |
|----|---|----|
| 1 | Classifying 1000 chips with 2% training set size. | 15 |
| 2 | Classifying 10000 chips with 2% training set size. | 16 |
| 3 | Kappa(cutoff) using t-excess thresholding. | 17 |
| 4 | Kappa(cutoff) using abs-t-excess thresholding. | 18 |
| 5 | z_{\max} using t-excess for thresholding. | 23 |
| 6 | z_{\max} using abs-t-excess for thresholding. | 24 |
| 7 | Quotient of z_{\max} averages and kappa. | 25 |
| 8 | $\frac{TP}{FP}$ over threshold t | 26 |
| 9 | z_{\max} predicting T2 defect state knowing only T1 measurements. | 32 |
| 10 | Kappa(cutoff) of the foregoing figure. | 33 |
| 11 | z_{\min} predicting T2 defect state knowing only T1 measurements. | 34 |
| 12 | Kappa(cutoff) of the foregoing figure. | 35 |

References

- [1] Salvador Abreu, Philippe Codognet, and Daniel Diaz. On the implementation of gnu prolog. *Theory and Practice of Logic Programming*, 12(1-2):253–282, 2012.
- [2] Alejandro Barredo Arrieta, Natalia Díaz-Rodríguez, Javier Del Ser, Adrien Bénéttot, Siham Tabik, Alberto Barbado, Salvador García, Sergio Gil-Lopez, Daniel Molina, Richard Benjamins, Raja Chatila, and Francisco Herrera. Explainable Artificial Intelligence (XAI): Concepts, taxonomies, opportunities and challenges toward responsible AI. *Information Fusion*, 58:82–115, 2020.
- [3] Jacob Cohen. A coefficient of agreement for nominal scales. *Educational and Psychological Measurement*, 20(1):37–46, 1960.
- [4] Dheeru Dua and Casey Graff. UCI machine learning repository, 2017.
- [5] Ronald Aylmer Fisher. The use of multiple measurements in taxonomic problems. *Annals of Eugenics*, 7(2):179–188, 1936.
- [6] Corrado Gini. Variabilità e mutabilità. Reprinted in: *Memorie di metodologia statistica* (Eds. E. Pizetti and T. Salvemini), Rome: Libreria Eredi Virgilio Veschi, 1955.
- [7] J. D. Hunter. Matplotlib: A 2d graphics environment. *Computing in Science & Engineering*, 9(3):90–95, 2007.
- [8] R. Kowalski. Algorithm = Logic + Control. *CACM*, 22(7):424–436, 1979.
- [9] D. E. Rumelhart, G. E. Hinton, and R. J. Williams. Learning representations by back-propagating errors. *Nature*, 323(6088):533–536, 1986.

- [10] John E. Savage. *Models of Computation: Exploring the Power of Computing*. Addison-Wesley, 1998.